Toxicon 112 (2016) 68–76

Contents lists available at ScienceDirect

Toxicon

journal homepage: www.elsevier.com/locate/toxicon

Identification of gymnodimine D and presence of gymnodimine variants in the dinoflagellate *Alexandrium ostenfeldii* from the Baltic Sea

Kirsi Harju [a, *], Harri Koskela [a], Anke Kremp [b], Sanna Suikkanen [b], Pablo de la Iglesia [c, 1], Christopher O. Miles [d, e], Bernd Krock [f], Paula Vanninen [a]

[a] VERIFIN, Department of Chemistry, P.O. Box 55, A. I. Virtasen aukio 1, FI-00014, University of Helsinki, Finland
[b] Finnish Environment Institute, Marine Research Centre, Erik Palménin aukio 1, FI-00560, Helsinki, Finland
[c] IRTA, Carretera de Poble Nou, km 5.5, 43540, Sant Carles de la Rápita, Spain
[d] Norwegian Veterinary Institute, P.O. Box 750 Sentrum, N-0106, Oslo, Norway
[e] Department of Pharmaceutical Chemistry, School of Pharmacy, University of Oslo, P.O. Box 1068 Blindern, N-0316, Oslo, Norway
[f] Alfred Wegener Institute, Am Handelshafen 12, D-27570, Bremerhaven, Germany

ARTICLE INFO

Article history:
Received 27 November 2015
Received in revised form
19 January 2016
Accepted 26 January 2016
Available online 29 January 2016

Keywords:
Gymnodimine
Dinoflagellate
Alexandrium ostenfeldii
Nuclear magnetic resonance
Liquid chromatography–mass spectrometry
High resolution mass spectrometry

ABSTRACT

Gymnodimines are lipophilic toxins produced by the marine dinoflagellates *Karenia selliformis* and *Alexandrium ostenfeldii*. Currently four gymnodimine analogues are known and characterized. Here we describe a novel gymnodimine and a range of gymnodimine related compounds found in an *A. ostenfeldii* isolate from the northern Baltic Sea. Gymnodimine D (**1**) was extracted and purified from clonal cultures, and characterized by liquid chromatography–tandem mass spectrometry (LC–MS/MS), nuclear magnetic resonance (NMR) spectroscopy, and liquid chromatography–high resolution mass spectrometry (LC–HRMS) experiments. The structure of **1** is related to known gymnodimines (**2**–**5**) with a six-membered cyclic imine ring and several other fragments typical of gymnodimines. However, the carbon chain in the gymnodimine macrocyclic ring differs from the known gymnodimines in having two tetrahydrofuran rings in the macrocyclic ring.

1. Introduction

Gymnodimines (GYMs) (Fig. 1) are cyclic imines produced by two species of marine planktonic dinoflagellates, *Karenia selliformis* and *Alexandrium ostenfeldii*. Gymnodimine A (**2**) was found first in New Zealand oysters in 1994 (Seki et al., 1995; Stewart et al., 1997), and since then, it has been detected in several other locations around the world, and supposedly produced by *K. selliformis*. The hydroxylated analogues, gymnodimine B (**3**) and C (**4**), have also been isolated from *K. selliformis* (Miles et al., 2000, 2003). These gymnodimines can be present in filter-feeding shellfish throughout the year, and have been detected in large quantities in coastal waters of New Zealand (Stirling, 2001) and Tunisia (Biré et al., 2002; Ben Naila et al., 2012) after prolonged blooms of *K. selliformis*. Recently, 12-methylgymnodimine (**5**) was isolated from *A. ostenfeldii* originating from estuaries at the U.S. East Coast, which was the first report of gymnodimines in *Alexandrium* or any other dinoflagellate species besides *K. selliformis* (Van Wagoner et al., 2011). Besides 12-methylgymnodimine isolated from an *A. ostenfeldii* strain from the U.S. East Coast, gymnodimine A and 12-methylgymnodimine have been found together with spirolides in isolates from a recent bloom of *A. ostenfeldii* in the Netherlands (Van de Waal et al., 2015). Moreover, novel fatty acid ester metabolites of gymnodimine A (de la Iglesia et al., 2013) and several unknown gymnodimine-like compounds (McCarron et al., 2014) have been detected in shellfish by liquid chromatography–mass spectrometry (LC–MS). Compared to other cyclic imines, such as the structurally related pinnatoxins (Aráoz et al., 2011) and spirolides (Guerét and Brimble, 2010), knowledge on gymnodimines is still limited. Gymnodimine A is a fast-acting toxin with high intraperitoneal toxicity in mice (LD_{50} of 80–96 μg/kg) (Kharrat

* Corresponding author. Tel.: +358 2941 50351; fax: +358 2941 50437.
E-mail address: kirsi.harju@helsinki.fi (K. Harju).
[1] Present address: Waters Cromatografía. Ronda de can Fatjó, 7-A. Parc Tecnològic del Vallès, E-08290 Cerdanyola del Vallés, Barcelona, Spain.

http://dx.doi.org/10.1016/j.toxicon.2016.01.064
0041-0101/

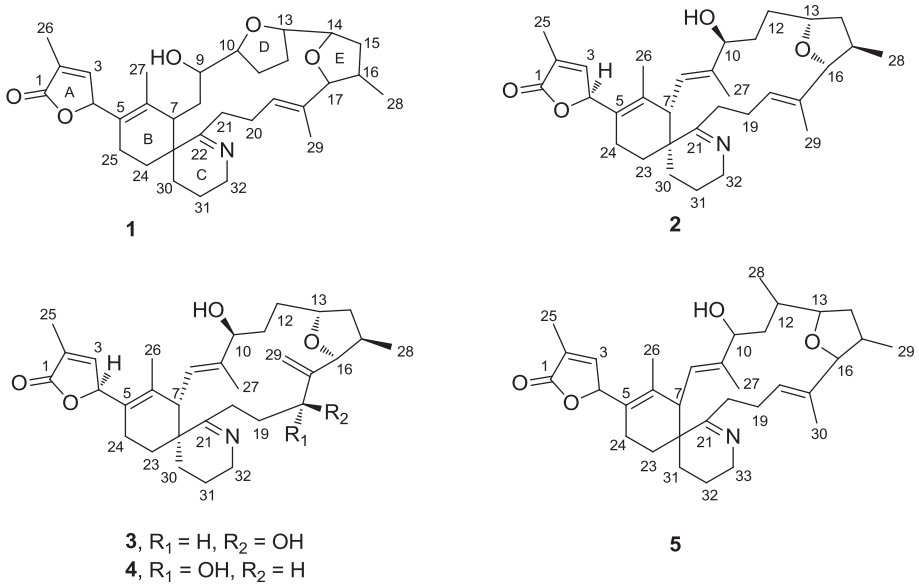

Fig. 1. The structures of gymnodimine D (1), gymnodimine A (2), gymnodimine B (3), gymnodimine C (4), and 12-methylgymnodimine (5).

et al., 2008; Munday et al., 2004) and similar bioactivities have been reported from other cyclic imines (Munday, 2008). Gymnodimine A is of low oral toxicity to mice, and is regarded as low risk for humans (Munday et al., 2004). Despite the high acute toxicity in mouse bioassays, cyclic imines are not currently regulated in seafood (EFSA Panel, 2010); and this is probably related to the fact that acute poisonings in humans could not be related directly to contamination of seafood with cyclic imines and the fact that potential effects from long-term exposure to subacute doses are not yet fully investigated. Cyclic imines show acetylcholine receptor binding activity with potential effects on the peripheral and central nervous system, and may have potential for the treatment of neurological disorders such as Alzheimer's disease (Molgó et al., 2014).

A wide variety of cyclic imines are known to be produced by phylogenetically distant dinoflagellates (Molgó et al., 2007). Pinnatoxins were first detected in seafood before the dinoflagellate *Vulcanodinium rugosum* was shown to be the causative organism of toxin production (Rhodes et al., 2010, 2011). Pinnatoxins E–H are produced by dinoflagellates (Selwood et al., 2010, 2014), whereas other known pinnatoxins and pteriatoxins (Takada et al., 2001) are thought to be formed in shellfish via metabolism of pinnatoxin F and G (Selwood et al., 2010). Recently portimine, a polycyclic ether with a five-membered cyclic imine ring, was isolated from a *V. rugosum* isolate (Selwood et al., 2013). Like pinnatoxins, spirolides were also first detected in shellfish (Hu et al., 1995). The causative organism of spirolide production was identified as *A. ostenfeldii* isolated in Nova Scotia, Canada and Limfjord, Denmark (Cembella et al., 2000). Spirolides A, C, and 13-desmethylspirolide C were isolated from *A. ostenfeldii* cultures (Nova Scotia, Canada) and their structures were determined (Hu et al., 2001). Subsequently, various spirolide analogues have been isolated and structurally characterized from *A. ostenfeldii* (Aasen et al., 2005; MacKinnon et al., 2006a; Roach et al., 2009; Ciminiello et al., 2010). Several unknown analogues have also been described together with known spirolides (Sleno et al., 2004; Almandoz et al., 2014; Tillmann et al., 2014; Rundberget et al., 2011). Certain *A. ostenfeldii* isolates may produce both spirolides and gymnodimines (Van Wagoner et al., 2011; Van de Waal et al., 2015). Due to their structural similarity, a possible explanation may be a common biosynthetic pathway.

A. ostenfeldii populations from the Baltic Sea produce paralytic shellfish poisoning (PSP) toxins, but spirolides have not yet been reported in these isolates (Kremp et al., 2014). Here we report detection of novel gymnodimines in an *A. ostenfeldii* isolate from a Baltic Sea bloom site, and the identification and structural characterization of gymnodimine D (**1**) from an *A. ostenfeldii* culture. Though the molecular formula was the same as for gymnodimine B and C, the mass spectrum of **1** was not fully consistent with gymnodimine B and C. Because the reference standards for gymnodimines B and C were not commercially available, the isolation of **1** was necessary for proper structural characterization.

2. Materials and methods

2.1. Reagents

A certified reference standard of gymnodimine A was purchased from the National Research Council (Halifax, Canada) and 12-methylgymnodimine was purchased from Biomol GmbH (Hamburg, Germany). Fractions of unidentified *A. ostenfeldii* gymnodimines were obtained from clonal isolate AOVA-0930 established as described (Tahvanainen et al., 2012) from material collected at the north coast of Gotland, Sweden, Baltic Sea (gene bank accession number of consensus ITS1-5.8S-ITS2, 28S sequences and partial saxitoxin sequence: JX841276, JX841302, KC835398).

2.2. Cell culture

Exponentially growing cells of AOVA-0930 were inoculated at an initial concentration of 500 cells/mL to thirty 250 mL tissue culture flasks (Nunc) each containing 160 mL of f/2-Si growth media (Guillard and Ryther, 1962) prepared from local 0.8 μm filtered sea water (salinity 6). The batch cultures were grown at 16 °C with 14:10 h light:dark cycle (50 μmol photons m^{-2} s^{-1}). Cell concentrations were monitored by regular microscopic cell counts. After 5 weeks, when cultures had reached stationary phase at cell concentrations of approximately 30,000 cells/mL, the contents of each culture flask (n = 30) was filtered on a separate glass microfiber filter (Whatman GF/C, Ø 47 mm), washed with Milli-Q water (3 × 3 mL), and freeze-dried for 24 h prior to extraction (n = 18).

The rest of the cell samples were stored in a freezer (−20 °C).

2.3. Sample preparation

The filter papers (n = 18) were extracted with methanol (4 mL). The extracts were filtered with syringe filters (0.45 μm, Millex), combined, and concentrated under nitrogen flow. The residue was dissolved in eluent from LC–MS/MS Method A (A–B 1:1, v/v), filtered with a centrifugal filter (PVDF 0.45 μm, Millipore), and the volume was adjusted to 2.0 mL, of which 500 μL and 900 μL were taken for the purification. This corresponds to approximately 22 and 40 million dinoflagellate cells. The sample was enriched with an Agilent 1200 HPLC system (Santa Clara, USA) connected diode-array detector and Bruker BPSU-36 peak sampling unit with storage loop volume of 250 μL. Concentrated AOVA-0930 extract was injected onto a Hypersil BDS C8 column (150 × 4.6 mm, 5 μm, Thermo Scientific, USA). The injection volume was 100 μL, and the injection was repeated five times for the preliminary NMR analyses in deuterated water. Additional nine injections of 100 μL was purified with Agilent 1200 HPLC system connected to Agilent G1364CR fraction collector for the NMR analyses of **1** in deuterated pyridine. Purification used a linear gradient (1 mL/min) of 2 mM ammonium formate and 50 mM formic acid in water (A) and acetonitrile (B), with 70% A for 2 min, then to 10% over 15 min followed by 2 min at 10% A, to 70% A over 0.1 min and then held at 10% A for 5.9 min. The fractions were collected on the basis of UV detection at 215 nm. The sample purity and identity in the separated fractions was confirmed with LC–MS/MS ($[M+H]^+$ at *m/z* 524) producing fragments *m/z* 506 (100%), *m/z* 496 (17–20%), and *m/z* 346 (37–46%) with the retention time shift within ±0.2 min. The collected fractions containing the major analogue were pooled (rt 8.50–9.75 min), concentrated with EZ-2 Plus evaporator (Genevac Ltd, Ipswich, UK), and analyzed by means of LC–MS/MS, LC–HRMS, and NMR.

2.4. LC–MS/MS method A

A Finnigan LXQ linear ion trap mass spectrometer with electrospray ionization (ESI) source interfaced to a Finnigan Surveyor Autosampler Plus Liquid Chromatograph (Thermo Scientific, San Jose, USA) was used for LC–MS/MS analyses. The compounds were separated on a Hypersil BDS C8 column (150 × 4.6 mm, 5 μm; Thermo Scientific) at a flowrate of 1000 μL/min, and an injection volume of 15 μL. Separation was performed with a mobile phase of 2 mM ammonium formate and 50 mM formic acid in water (A) and acetonitrile (B) using a linear gradient from 70% A to 10% A as described for the sample purification. The eluent flow was split 1:20 to the mass detector. Positive mode electrospray ionization was applied with spray voltage 5 kV, capillary temperature 300 °C, capillary voltage 30 V, sheath gas 30, auxiliary gas 15. A scan range of *m/z* 50–900 was used for screening, and MS/MS at $[M+H]^+$ *m/z* 524 for **1** and 508 for gymnodimine A.

2.5. LC–MS/MS method B

A triple quadrupole 3200 QTrap MS with a TurboV electrospray ionization source (AB/Sciex, Foster City, CA) hyphenated to an Agilent 1200 LC system (Agilent Tech., Santa Clara, CA) was used for additional LC–MS/MS analyses. The compounds were separated on an X-Bridge C8 column (2.1 mm × 50 mm, 3.5 μm; Waters Corp.) at a flowrate of 500 μL/min, and an injection volume of 10 μL under alkaline conditions according to previously reported conditions (Gerssen et al., 2009; García-Altares et al., 2013). Briefly, mobile phase A consisted of 6.7 mM of ammonium hydroxide in ultrapure Milli-Q water. Mobile phase B consisted of 6.7 mM of ammonium hydroxide in 90/10 (v/v) acetonitrile/Milli-Q water. The gradient ran from 20 to 100% B over 8 min, held at 100% B for 1 min, returned to the initial conditions over the next 0.5 min, and finally held at the starting conditions for equilibration until a total run cycle of 12 min. Positive polarity MS mode was applied with the following collision and source parameters: 20 psi curtain gas, 5500 V ion spray voltage, 500 °C nebuliser gas temperature, 50 psi nebuliser and heater gases, level 4 (arbitrary units) collision-activated dissociation gas and 55 eV collision energy and 2600 V continuous electron multiplier. Enhanced product ion spectra (EPI) were acquired in the range *m/z* 150–525, from the precursor ion *m/z* 524.3 for **1**. The spectra obtained for 1 were compared with those obtained from the certified reference material of gymnodimine A at *m/z* 508.3.

2.6. LC–HRMS method C

Liquid chromatography was performed with a Waters Acquity UPLC pump and autosampler on a Symmetry C18 column (3.5 μm, 100 × 2.1 mm; Waters, Milford, MA, USA) eluted with a linear gradient (0.3 mL/min) of acetonitrile (A) and water (B), each containing 0.1% formic acid. The gradient was from 15 to 65% A over 11 min, to 95% A at 11.5 min (1 min hold), followed by a return to 15% A at 13 min with a 3-min hold to equilibrate the column. A Q Exactive mass spectrometer (Thermo Scientific, Bremen, Germany) was used as detector, with spray voltage 3.5 kV, capillary temperature 350 °C, probe heater 300 °C, S-lens RF level 50, with sheath and auxiliary gas 35 and 10, respectively. The spectrometer was operated in positive all-ion-fragmentation (AIF) mode (full scan: scanned *m/z* 400–900, AGC target 5×10^6, resolution 70,000, and max IT 200 ms; AIF scanned *m/z* 110–1500, AGC target 3×10^6, resolution 35,000, max IT 200 ms, and normalized collision energy 30).

2.7. NMR analyses

For NMR analyses in deuterated water, the pooled sample after EZ-2 Plus evaporation (Genevac Ltd, Ipswich, UK) was concentrated to 500 μL under nitrogen flow. Deuterium oxide (D_2O) was added (100 μL), and the sample volume of 600 μL was adjusted into the NMR 5 mm tube. The sample in deuterated water was further concentrated into the volume of 30 μL for the NMR analyses with a 1.7 mm microcoil probe. The second NMR microprobe sample from the purification of AOVA-0930 (9 × 100 μL injections) was evaporated to dryness with EZ-2 Plus evaporator (Genevac Ltd, Ipswich, UK) and dissolved in deuterated pyridine. The final volume of the microprobe NMR sample (30 μL) was adjusted in a total recovery vial (12 × 32 mm, glass, screw neck, p/n 6000000750cv, Waters, Milford, MA, U.S.A.) before transfer to the microprobe sample tube (part no. Z106463, Bruker Biospin, Rheinstetten, Germany). The deuterated water sample in a 5 mm NMR tube was measured with a Bruker Avance III HD 850 MHz NMR spectrometer equipped with a 5 mm TCI (^1H, ^{13}C, ^{15}N) cryoprobe, and both microprobe samples were recorded with a Bruker Avance III 500 MHz NMR spectrometer equipped with a 1.7 mm TXI (^1H, ^{13}C, ^{31}P) microcoil probe. The measurement temperature was 290 K. Proton chemical shift referencing in deuterated water samples was performed against external 4,4-dimethyl-4-silapentane-1-sulfonic acid, and in deuterated pyridine samples using the residual solvent peaks. Carbon chemical shift referencing was performed with Ξ calibration (Harris et al., 2008). The chemical shifts in the Table 1 were obtained with 500 MHz NMR spectrometer in deuterated pyridine. The comparison of the data obtained in deuterated water is presented in the supporting information. The concentrated fraction in a 5 mm NMR tube contained 2% formic acid, 0.2% ammonium formate and a trace amount of glycerol, but no other significant

Table 1
NMR Spectroscopic Data for 1 (500 MHz, pyridine-d_5).

Position	δ_C, type	δ_H (mult; *J* in Hz)	HMBC (C)[a]
1	175.2, C		
2	130.2, C		
3	148.5, CH	6.96 (quint.; 1.6)	1, 2, 4, 26
4	81.1, CH	5.95 (m)	2, 3, 5, 6, 25
5	125.7, C		
6	137.4, C		
7	44.2, CH	3.09 (m)	5, 6
8	30.9, CH_2	1.43 (m) (H_a)	6
		1.82 (m) (H_b)	6, 7, 9, 10, 23
9	72.5, CH	3.96 (m)	7, 10, 11
10	84.3, CH	4.02 (m)	8, 9, 12, 13
11	28.4, CH_2	1.85 (m) (H_a)	12, 13, 14
		1.99 (m) (H_b)	9, 12, 13
12	25.9, CH_2	1.85 (m)	11
13	80.3, CH	4.27 (td; 10.5, 2.9)	10, 14
14	78.7, CH	4.09 (m)	12, 16
15	34.5, CH_2	1.22 (m) (H_a)	13, 14, 16, 28
		1.91 (m) (H_b)	13, 16, 17, 28
16	36.0, CH	2.30 (sept.; 7.0)	14, 15, 18, 28
17	84.5, CH	4.09 (m)	14, 16, 18, 19, 28, 29
18	129.7, C		
19	127.8, CH	5.98 (t; 5.9)	17, 21, 29
20	21.8, CH_2	2.14 (m) (H_a)	19, 22
		3.00 (t; 11.6) (H_b)	19
21	32.1, CH_2	2.38 (m) (H_a)	
		2.64 (m) (H_b)	22
22	172.8, C		
23	43.5, C		
24	33.6, CH_2	1.33 (m) (H_a)	5, 7, 22, 23, 25, 30
		1.64 (m) (H_b)	5, 22, 23, 30
25	19.8, CH_2	1.53 (m) (H_a)	
		1.93 (m) (H_b)	
26	10.7, CH_3	1.96 (t; 1.6)	1, 2, 3, 4
27	17.9, CH_3	2.06 (s)	5, 6, 7
28	16.7, CH_3	0.86 (d; 7.1)	15, 16, 17
29	15.4, CH_3	1.56 (s)	17, 18, 19
30	26.9, CH_2	1.44 (m) (H_a)	7, 22, 23
		1.52 (m) (H_b)	23, 24, 31, 32
31	20.3, CH_2	1.44 (m)	32
32	50.1, CH_2	3.51 (m) (H_a)	
		3.73 (m) (H_b)	

[a] HMBC correlations are stated from protons to the indicated carbons.

impurities. The sample in deuterated pyridine contained approximately 0.5% formic acid and ammonium formate but no other significant impurities. Apart from EASY-ROESY (Thiele et al., 2009), the NMR experiments were acquired using Bruker's Topspin standard pulse sequences. J_{HH} couplings from clearly resolved multiplets have been determined with PERCH spectral simulation software (PERCH Solutions Ltd., version 2013.1). The yield of **1** was calculated with an external standard of methylphosphonic acid in H_2O/D_2O using the PULCON method (Wider and Dreier, 2006) implemented in the ERETIC2 quantification of the Bruker Topspin software.

3. Results and discussion

A. ostenfeldii is a microalga, which is known to produce several different phycotoxins (Kremp et al., 2014). The reasons for such diversity and the observed variation of toxin profiles among isolates is not clear though a relationship between toxin composition, phylogenetic position and habitat type has been indicated. The geographic origin also affects the toxin profile (Salgado et al., 2015). The production of PSP toxins is predetermined and dependent on the presence of specific saxitoxin gene motifs (Suikkanen et al., 2013). The genetic basis for cyclic imine production is presently not very well understood. Previously it was found that *A. ostenfeldii* isolates from U.S East Coast estuaries and brackish coastal waters in the Netherlands produce both PSP toxins and cyclic imines, spirolides as well as various gymnodimines (Van Wagoner et al., 2011; Van de Waal et al., 2015). The respective isolates are phylogenetically closely related to *A. ostenfeldii* populations from the Baltic Sea (Kremp et al., 2014), which motivated us to search for gymnodimines in Baltic *A. ostenfeldii* cultures. A major (**1**) and minor gymnodimine B/C-like compound with $[M+H]^+$ at *m/z* 524 were detected by LC–MS/MS in *A. ostenfeldii* isolate AOVA-0930 from the Baltic Sea (Fig. 2). The major compound was isolated and enriched from cultured cells, purified, and structurally characterized using LC–MS/MS, LC–HRMS, and NMR studies.

Accurate masses (Table 3) of **1** and the minor gymnodimine were consistent with the molecular formula for gymnodimine B/C, $C_{32}H_{45}O_5N$ (with 11 rings or double bond equivalents), previously isolated from *K. selliformis* (Miles et al., 2000, 2003). However, the mass spectrometric fragmentation patterns differed from those expected for gymnodimine B/C based on reports from literature (Ben Naila et al., 2012). Several product ions, such as *m/z* 496, 346, and 316 (Fig. 3), which did not match with the product ions expected for gymnodimine B/C, were detected in the product ion spectrum of **1**. Only very small product ions typical for gymnodimine B and C at *m/z* 488 and 202 were observed in the LC–MS/MS spectrum of **1**.

The structure of **1** (Fig. 1) was resolved by NMR spectroscopy and mass spectrometry. It is closely related to the known gymnodimines (**2**–**5**), and contains many structural features present in **2**–**5**, such as six-membered cyclic imine, butenolide, and tetrahydrofuran ring structures. The structure of **1** differs from gymnodimine A only between C-7 and C-14 of **1** (Fig. 1).

3.1. NMR analyses

The structure of **1** was determined by NMR experiments with 500 MHz and 850 MHz NMR spectrometers. The 500 MHz NMR spectroscopic data from deuterated pyridine sample is summarized in Tables 1 and 2. The through-bond connectivities of protons

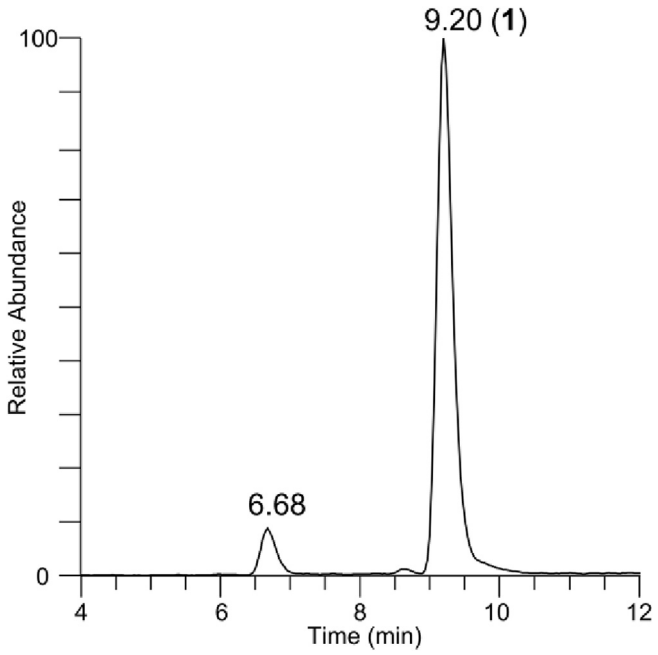

Fig. 2. LC–MS/MS (method A) total ion chromatogram of product ion scan of $[M+H]^+$ at *m/z* 524 of *A. ostenfeldii* strain AOVA-0930.

Table 2
Proton–proton COSY and TOCSY correlations and spatial NOESY connections for 1 (500 MHz, pyridine-d_5).

Position	δ_H	COSY (H)	TOCSY (H)	NOESY (H)
3	6.96	4, 26		4, 25_a, 27
4	5.95	3, 26	7	3, 26, 27
7	3.09	8_{ab}	4, 9, 10, 13, 27	9, 21_b, 24_b, 25_a, 27
8	1.43 (H_a)	7, 8_b, 9		
	1.82 (H_b)	7, 8_a, 9		10, 27
9	3.96	8_{ab}, 10	7, 11_b, 12, 13, 27	7, 19
10	4.02	9, 11_a, 12,	7, 13	8_b, 11_b, 19
11	1.85 (H_a)	10, 11_b	13	19
	1.99 (H_b)	10, 11_a,	9, 12, 13	10
12	1.85	13	9, 10, 11_b	19
13	4.27	12, 14	9, 10, 11_{ab}, 15_a, 16, 28	10, 12, 14
14	4.09	13, 15_{ab}	17	13, 15_b, 17
15	1.22 (H_a)	14, 15_b, 16	13, 17, 28	28
	1.91 (H_b)	14, 15_a, 16	17, 28	14, 16
16	2.30	14, 15_{ab}, 28	13, 17	15_b, 28, 29
17	4.09	16, 19, 29	14, 15_{ab}, 20_{ab}, 21_{ab}, 28	14, 16, 29
19	5.98	17, 20_{ab}, 29	21_a, 21_b, 32_{ab}	9, 10, 12, 20_b
20	2.14 (H_a)	19, 20_b 21_{ab}, 29	17, 32_{ab}	29
	3.00 (H_b)	19, 20_a, 21_b, 29,	17, 21_a, 32_{ab}	19, 29
21	2.38 (H_a)	20_a, 21_b	17, 19, 20_b, 32_{ab}, 29	
	2.64 (H_b)	20_{ab}, 21_a	17, 19, 29, 32_{ab}	7, 19
24	1.33 (H_a)	24_b, 25_b	25_a, 27, 30	
	1.64 (H_b)	24_a, 25_{ab}	27	7
25	1.53 (H_a)	24_b, 27	24_a	7
	1.93 (H_b)	24_{ab}	7, 25_a, 27	
26	1.96	3, 4		4
27	2.06	7, 25_a	9, 10, 24_{ab}, 25_b, 30_b	3, 4, 7, 8_b
28	0.86	16	13, 15_{ab}, 17	15_a, 16, 29
29	1.56	17, 19, 20_{ab}	21_{ab}	16, 17, 20_{ab}, 28
30	1.44		32_b	
	1.52		24_{ab}, 25_b, 27, 32_b	24_b
31	1.44	32_a, 32_b		32_a
32	3.51 (H_a)	32_b	19, 20_{ab}, 21_{ab}	31
	3.73 (H_b)	31, 32_a	19, 20_{ab}, 21_{ab}, 30_a	

Table 3
Exact and Measured Accurate Masses (m/z) for $[M+H]^+$ at m/z 524 and Its Product Ions Obtained with LC–HRMS (Method C).

Formula	Calculated	Measured	Δ (ppm)
$C_{32}H_{46}NO_5^+$	524.3371	524.3365	−1.0
$C_{32}H_{44}NO_4^+$	506.3265	506.3262	−0.5
$C_{31}H_{46}NO_4^+$	496.3421	496.3430	2.0
$C_{32}H_{42}NO_3^+$	488.3159	488.3149	−2.0
$C_{31}H_{46}NO_3^+$	480.3472	480.3466	−1.2
$C_{31}H_{44}NO_2^+$	462.3367	462.3357	−2.1
$C_{27}H_{40}NO_3^+$	426.3003	426.2997	−1.2
$C_{27}H_{38}NO_2^+$	408.2897	408.2886	−2.8
$C_{24}H_{36}NO_4^+$	402.2639	402.2629	−2.5
$C_{21}H_{32}NO_3^+$	346.2377	346.2377	0.0
$C_{20}H_{30}NO_2^+$	316.2271	316.2263	−2.5
$C_{15}H_{24}N^+$	218.1903	218.1900	−1.5
$C_{14}H_{22}N^+$	204.1747	204.1745	−1.1
$C_{14}H_{20}N^+$	202.1590	202.1586	−2.4
$C_{11}H_{16}N^+$	162.1277	162.1277	−0.5
$C_9H_{14}N^+$	136.1121	136.1121	−0.5

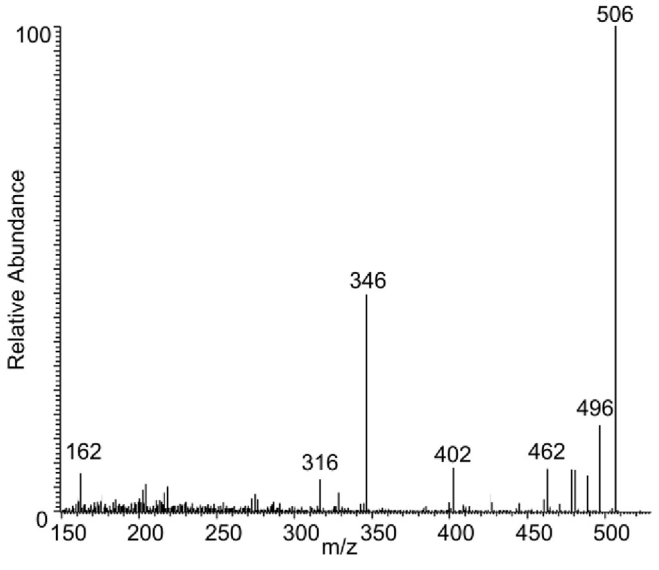

Fig. 3. Product ion spectrum of 1 obtained by LC–MS/MS (method A), $[M+H]^+$ at m/z 524 in the range m/z 150–530.

within the chain were observed with the correlation spectroscopy (COSY) and total correlation spectroscopy (TOCSY) experiments, and spatial closeness was determined using NOESY (nuclear Overhauser spectroscopy) or rotating-frame nuclear Overhauser spectoroscopy EASY–ROESY experiment (Thiele et al., 2009). Protonated and quaternary carbons were assigned indirectly with the multiplicity-edited HSQC (heteronuclear single quantum correlation) and HMBC (heteronuclear multiple bond correlation) experiments, respectively. The preliminary studies were performed in deuterated water with an 850 MHz NMR spectrometer equipped with a 5 mm cryoprobe. The imine carbon (C-22, C=N) was not detected due to signal broadening under acidic conditions and deuterium exchange. In addition, an overlap of C-23 and C-32 was observed in deuterated water. More gymnodimine D was isolated and the NMR spectra were recorded in deuterated pyridine with a 500 MHz NMR spectrometer equipped with a microcoil probe. Imine carbon could be detected and C-23 and C-32 were differentiated in deuterated pyridine. In addition, more connectivities were

seen because of higher sample concentration. The observed ^{1}H and ^{13}C ppm values were similar to the values measured for the corresponding functional groups of gymnodimine A (**2**) (Seki et al., 1995) and 12-methylgymnodimine (**5**) (Van Wagoner et al., 2011). The comparison of the chemical shifts for **1**, **2**, and **5** is presented in the supporting information (Table S1).

Gymnodimine D (**1**) had only four methyl groups, rather than the five in **2**, and had an additional CH_2 group (C-8) in the macrocyclic ring. Only one carbon double bond (C=C) was identified in the macrocyclic ring, compared to two double bonds in other gymnodimines. An exocyclic methylene ($C{=}CH_2$) such as is present in **3** and **4**, was not present in **1**.

HMBC correlations from H-4, H-7, H-24_{ab}, and H-27 to C-5 in ring B were observed. Additionally, connections to spirocyclic C-23 were detected from H-8_b, H-24_{ab}, and H-30_a; and correlation of H-30_b to C-24 and H-24_{ab} to C-30 in HMBC demonstrates that rings B and C are connected. HMBC connections to imine carbon (C-22) were detected from H-20_a, H-21_b, H-24_{ab} and H-30_a, when the sample was analyzed in deuterated pyridine.

The HMBC correlations of H-3 and H-4 to carbons in the butenolide ring (A) as well as the correlation of H-4 to the adjacent C-5, C-6, and C-25 were detected. Moreover, the NOESY experiment showed spatial proximity between H-4 and 27-methyl protons. In addition to the two oxygens in the butenolide ring, LC–HRMS indicated that **1** had three more oxygen atoms. Five –CH–O– groups were detected in the NMR experiments in the same spin system. Four –CH–O– carbon resonances with approximately the same ppm values were attributable to two tetrahydrofuran rings (C-10, C-13, C-14, and C-17). HMBC spectra showed the connectivities from H-10 to C-13 and H-17 to C-14 over the oxygen bridges. Further proof of the tetrahydrofuran ring structures was obtained with NOESY experiment (Fig. 4). The NOESY experiments revealed that the H-14 and H-17 (ring E) as well as H-10 and H-13 (ring D) were on the same side of their tetrahydrofuran rings, and that H-9 is spatially close to H-10. In addition, NOESY correlations between H-14 and H-15_b and between H-16 and H-17 were detected. The low value of $^{3}J_{13,14}$ (3.2 Hz) indicated a gauche conformation between these protons.

The NOESY experiments showed that the methyl group (C-28) in the tetrahydrofuran ring is on the opposite side of the ring compared to gymnodimine A (Fig. 4). The NOESY correlation from methyl protons (H-28) was seen only to H-15_a, but not to H-14, H-15_b, or H-17. A strong NOESY correlation between H-28 and H-29 was also observed, which indicates that these methyls are in close proximity in the structure.

The NOESY correlation between H-20_{ab} to H-29 and the chemical shift for C-29 (15.4 ppm) indicate an *E* configuration of the double bond. A similar chemical shift was reported for the corresponding methyl substituent in 12-methylgymnodimine (C-30, 14.9 ppm; Van Wagoner et al., 2011). The NOESY experiment showed also a spatial closeness of H-9, H-10, H-11_a, and H-12 to H-19, which suggests the folding of the gymnodimine macrocyclic ring so that these protons are close to each other.

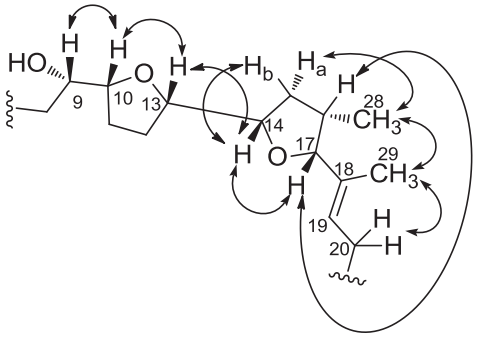

Fig. 4. The NOESY correlations of protons in the tetrahydrofuran rings (D and E).

Five injections of 100 μL of concentrated AOVA-0930 extracts yielded approximately 100 μg of **1**. Additional isolation of **1** with nine injections of the same AOVA-0930 extract was determined to contain 6.7 mg/mL of **1** in the microprobe sample volume of 30 μL indicating the yield of 200 μg.

3.2. LC–HRMS measurements

When the mass fragmentation pattern of **1** was studied, the high resolution product ion spectrum of $[M+H]^+$ at *m/z* 524 showed signals consistent with the structure derived from the NMR experiments (Table 3, Fig. 5). The most intense signal at *m/z* 506.3262 was caused by the loss of water ($[M + H{-}H_2O]^+$), while the other signals were weaker. Several fragments can be explained by retro Dies–Alder opening of the spirocyclic imine ring structure. Fragments typical for the cyclic imine moiety were clearly detected at *m/z* 136.1121 and 162.1277. An intense signal from **1** was observed at *m/z* 346.2377, matching with the formula of $C_{21}H_{32}NO_3^+$, and an additional loss of CH_2O produced a signal at *m/z* 316.2263. The loss of butenolide ring moiety is characteristic for gymnodimine A, clearly detected in the mass spectrum of gymnodimine A after the loss of water at *m/z* 392. Weak fragments at *m/z* 426 and 408 were seen in LC–MS/MS (Method B, Fig. S28) and at *m/z* 426.2997 and *m/z* 408.2886 in the LC–HRMS spectra (Table 3) of **1** consistent with the loss of butenolide followed by the loss of water, and it is likely that the cleavage at the secondary alcohol group position (C-9) in **1** is favoured. In addition, fragments at *m/z* 496.3430 and 480.3466 result from the losses of carbon monoxide (CO) and carbon dioxide (CO_2), respectively. A fragment at *m/z* 402.2629 in the LC–HRMS spectrum of **1** was consistent with a formula of $C_{24}H_{36}NO_4^+$, which corresponds to the loss of $C_8H_{10}O$. This fragment is proposed to be formed via other bond cleavages than the retro Diels–Alder.

3.3. Biosynthesis

The biosynthesis of several marine toxins by dinoflagellates is thought to occur via the formation of polyketides, but only limited information is available on the biosynthesis of cyclic imines (Kellmann et al., 2010; Van Wagoner et al., 2014). The biosynthesis of spirolides is based on the polyketide biogenetic pathway (MacKinnon et al., 2006b). It is also possible that these organisms contain two separate but closely related cyclic imine synthases. The homologation of one carbon in the macrocyclic ring of **1** differs from the other gymnodimines. The identified polyether-type structure in **1** has not been previously described for cyclic imines. Interestingly, a related structure with two tetrahydrofurans has been found e.g. in the iriomoteolide macrolide isolated from the marine dinoflagellate *Amphidinium* (Akakabe et al., 2014). Some bacterial polyethers, such as monensin, have a polyether structure, which is suggested to be formed through the cascade of cyclization reactions via epoxide ring structures. A related bis-ether structure is also thought to be an intermediate before the formation of bridged ketal structure in pectenotoxins produced by dinoflagellates (Van Wagoner et al., 2014). The ether ring-formation of two tetrahydrofuran rings in **1** occurs tentatively via 5-exo-tet reaction instead of 6-endo-tet ring-formation, which is favoured in the formation of ladder polyether toxins such as brevetoxins and yessotoxins (Vilotijevic and Jamison, 2010). A possible mechanism for formation of **1** is presented in Fig. 6, which shows the ring closure of butenolide, formation of spiroimine structure via Diels–Alder cyclization, and cyclization of tetrahydrofuran rings via epoxides.

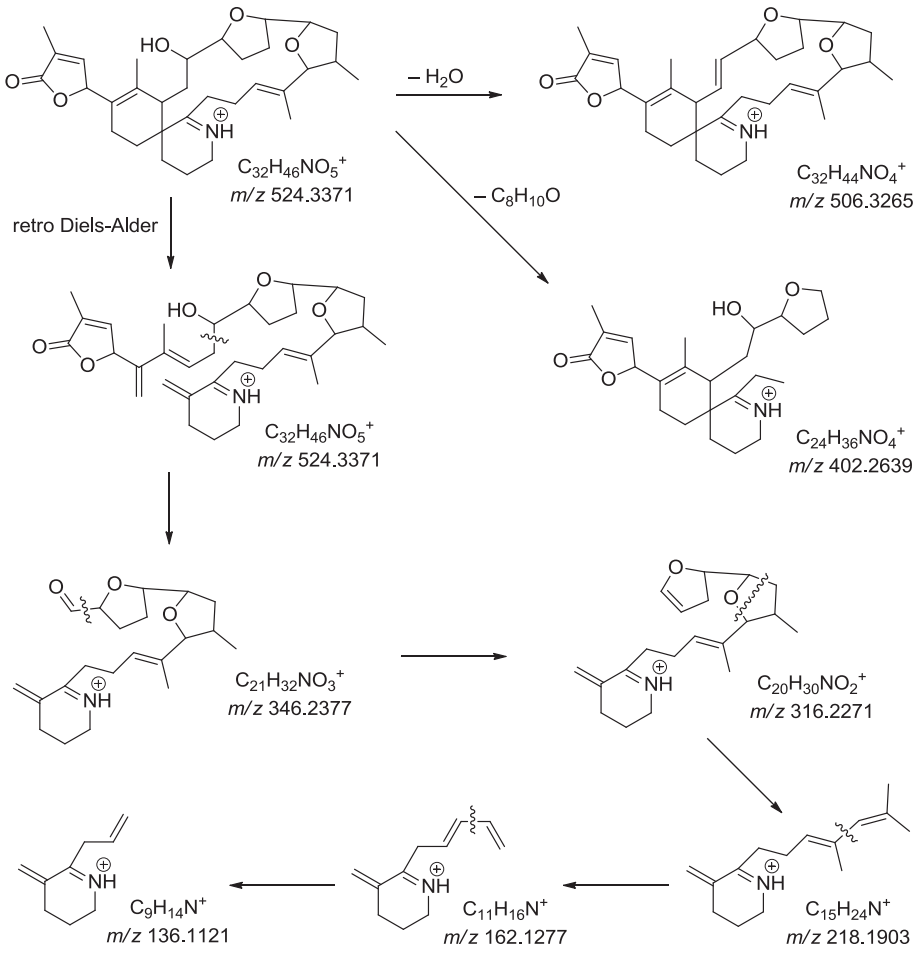

Fig. 5. Proposed structures of product ions of 1 with their corresponding formulae and exact masses.

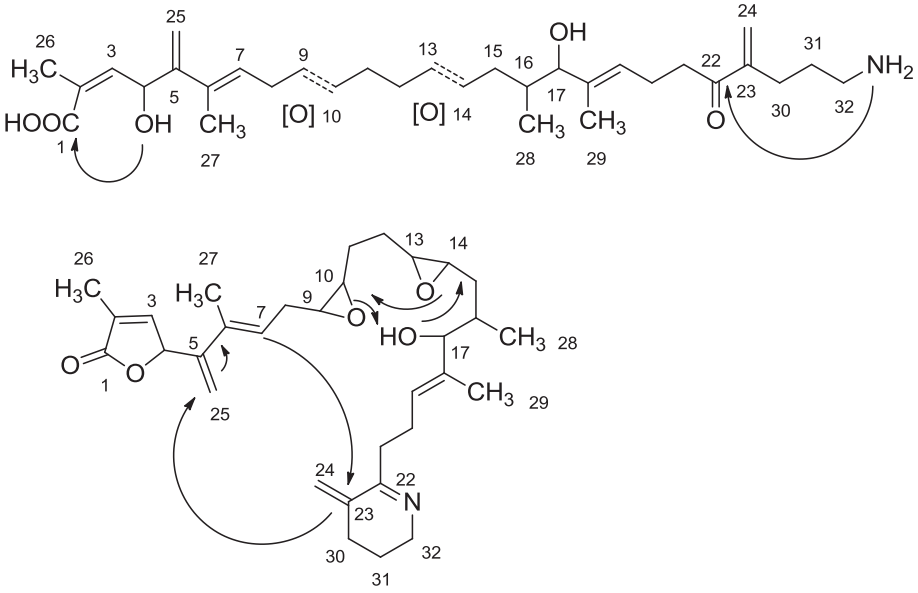

Fig. 6. Possible route for the formation of 1 via the epoxidation of a polyketide chain followed by the exocyclic ring formation of tetrahydrofuran structures.

3.4. Other gymnodimine analogues

More than 30 related gymnodimine-like compounds were detected when the highly concentrated, crude extract of AOVA-0930 was analyzed by LC–HRMS (method C) in the full scan mode and all-ion fragmentation (AIF) mode monitoring the fragment ion at *m/z* 136.1121 (Table 4 and Figs. S30–S35). The compounds were considered to be probable gymnodimine analogues if their peaks gave $[M+H]^+$ *m/z* 500–600 in full scan, the formulae contained one nitrogen atom, and had 9.5–10.5 ring or double bond equivalents (RDBE). The detected compounds contained one nitrogen atom, 31–35 carbons and 4–6 oxygens and varying numbers of hydrogens. Four pairs of compounds differing with two mass units (*m/z* 508/510, 524/526, *m/z* 540/542, and 582/584) were observed, which could indicate the butenolide double bond variation of the analogues, which is typical for spirolides (Fig. S32) (Hu et al., 2001). Moreover, six sodium adducts were detected with the same retention time as measured for $[M+H]^+$. Most of these compounds were only found at trace levels, too low to allow isolation and identification. Only $[M+H]^+$ at *m/z* 508.3425 (Table 4, entry 30), 524.3368 (Table 4, entry 5), 524.3359 (**1**, Table 4, entry 23), and 582.3788 (Table 4, entry 15) were clearly detected with ion trap instrument (LC–MS/MS, method A) from the diluted crude extract. 12-Methylgymnodimine ($[M+H]^+$ at *m/z* 522) was not seen in the full scan screening of the AOVA-0930 extract. A gymnodimine A -like compound ($[M+H]^+$ at *m/z* 508) was found with the same molecular formula as gymnodimine A, but the LC–MS/MS retention time and mass spectrum did not match with those of gymnodimine A.

Table 4
Putative Gymnodimines Detected by LC–HRMS (Method C) in an extract of *A. ostenfeldii* strain AOVA-0930. Entry 23 with the retention time (rt) of 7.34 min corresponds to 1.

Entry	rt (min)	*m/z*	Formula	Δ (ppm)	RDBE	Abundance (%)[a]
1	3.65	510.3217	$C_{31}H_{44}O_5N^+$	0.5	10.5	1.30
2	3.90	540.3324	$C_{32}H_{46}O_6N^+$	0.7	10.5	0.12
3	4.30	540.3323	$C_{32}H_{46}O_6N^+$	0.7	10.5	0.12
4	4.49	540.3323	$C_{32}H_{46}O_6N^+$	0.6	10.5	0.13
5	5.17	524.3368	$C_{32}H_{46}O_5N^+$	−0.4	10.5	7.60
6	5.33	540.3325	$C_{32}H_{46}O_6N^+$	1.3	10.5	0.04
7	5.46	540.3325	$C_{32}H_{46}O_6N^+$	1.0	10.5	0.07
8	5.65	526.3535	$C_{32}H_{48}O_5N^+$	1.5	9.5	0.05
9	5.73	542.3481	$C_{32}H_{48}O_6N^+$	0.9	9.5	0.21
10	5.88	540.3325	$C_{32}H_{46}O_6N^+$	1.0	10.5	0.33
11	6.08	542.3482	$C_{32}H_{48}O_6N^+$	1.0	9.5	0.13
12	6.26	582.3794	$C_{35}H_{52}O_6N^+$	0.9	10.5	0.03
13	6.36	524.3378	$C_{32}H_{46}O_5N^+$	1.3	10.5	0.08
14	6.43	542.3481	$C_{32}H_{48}O_6N^+$	1.0	9.5	0.19
		564.3301	$C_{32}H_{47}O_6NNa^+$	0.9		
15	6.45	582.3788	$C_{35}H_{52}O_6N^+$	−0.2	10.5	5.50
		604.3602	$C_{35}H_{51}O_6NNa^+$	−1.1		
16	6.54	524.3376	$C_{32}H_{46}O_5N^+$	1.1	10.5	0.07
17	6.64	540.3324	$C_{32}H_{46}O_6N^+$	0.9	10.5	0.26
18	6.76	524.3376	$C_{32}H_{46}O_5N^+$	1.1	10.5	0.44
19	6.91	526.3536	$C_{32}H_{48}O_5N^+$	1.7	9.5	0.04
20	7.05	584.3951	$C_{35}H_{54}O_6N^+$	0.8	9.5	0.12
21	7.08	582.3797	$C_{35}H_{52}O_6N^+$	1.3	10.5	0.04
		604.3615	$C_{35}H_{51}O_6NNa^+$	1.0	10.5	
22	7.21	540.3325	$C_{32}H_{46}O_6N^+$	0.9	10.5	0.13
23	7.34	524.3359	$C_{32}H_{46}O_5N^+$	−2.1	10.5	100.00
24	7.34	582.3782	$C_{35}H_{52}O_6N^+$	−1.3	10.5	0.10
		604.3622	$C_{35}H_{51}O_6NNa^+$	2.1		
25	7.71	526.3534	$C_{32}H_{48}O_5N^+$	1.3	9.5	0.31
26	7.86	526.3543	$C_{32}H_{48}O_5N^+$	3.0	9.5	0.05
27	7.89	540.3324	$C_{32}H_{46}O_6N^+$	0.8	10.5	0.18
28	8.13	524.3378	$C_{32}H_{46}O_5N^+$	1.4	10.5	0.09
29	8.29	508.3428	$C_{32}H_{46}O_4N^+$	1.4	10.5	0.05
30	8.55	508.3425	$C_{32}H_{46}O_4N^+$	0.7	10.5	8.90
31	8.92	510.3586	$C_{32}H_{48}O_4N^+$	1.7	9.5	0.13
32	9.13	510.3588	$C_{32}H_{48}O_4N^+$	2.0	9.5	0.02
33	9.38	542.3482	$C_{32}H_{48}O_6N^+$	1.0	9.5	1.70
		564.3300	$C_{32}H_{47}O_6NNa^+$	0.8		
34	9.89	526.3536	$C_{32}H_{48}O_5N^+$	1.7	9.5	0.16
		548.3353	$C_{32}H_{47}O_5NNa^+$	1.2		

[a] Relative abundances were estimated from the areas of the $[M+H]^+$ (and $[M-H+Na]^+$, where appropriate) peaks for the analogues relative to the peak for **1**.

4. Conclusions

In summary, the investigated Baltic Sea strain AOVA-0930 of *A. ostenfeldii* produces a combination of saxitoxins and gymnodimines. A new type of gymnodimine (**1**) was isolated from culture and characterized with LC–MS/MS, LC–HRMS, and NMR experiments. The novel structure containing two tetrahydrofuran rings in the macrocyclic ring has not been previously described for gymnodimines. Approximately 5 pg/cell of **1** was obtained from both purifications. The strain produces also saxitoxin and gonyautoxins 2 and 3. The total PSP toxin production of the strain has been measured to be 1.4–6.4 pg/cell under similar conditions, and the percentage of saxitoxin is about 50% of the PSP toxins (Suikkanen et al., 2013; Kremp et al., 2016). The diversity of gymnodimines revealed in this study indicates that further work is required in order to comprehensively identify and monitor these toxins in marine samples, and to evaluate their toxicity and environmental impacts.

Acknowledgments

This study was funded by the Academy of Finland (projects 251609, 128833, 251564, and 259357). The research leading to these results has received funding from the European Seventh Framework Programme (FP7/2007–2013) under the ECsafeSEAFOOD project (grant agreement no 311820). IRTA also acknowledges funding from the Spanish National Institute for Agricultural Research (INIA), through the project RTA 2013-00096-00-00.

Perttu Permi, Hideo Iwai, and Tuomas Niemi-Aro (Institute of Biotechnology, University of Helsinki, Finland) are thanked for the opportunity to use 850 MHz NMR instrument. The authors thank funding from Biocenter Finland for the NMR core facility at the Institute of Biotechnology.

Appendix A. Supplementary data

Supplementary data related to this article can be found at http://dx.doi.org/10.1016/j.toxicon.2016.01.064.

Transparency document

Transparency document related to this article can be found online at http://dx.doi.org/10.1016/j.toxicon.2016.01.064

References

Aasen, J., MacKinnon, S.L., LeBlanc, P., Walter, J.A., Hovgaard, P., Aune, T., Quilliam, M.A., 2005. Detection and identification of spirolides in Norwegian shellfish and plankton. Chem. Res. Toxicol. 18, 509–515.

Akakabe, M., Kumagai, K., Tsuda, M., Konishi, Y., Tominaga, A., Tsuda, M., Fukushi, E., Kawabata, J., 2014. Iriomoteolide-13a, a cytotoxic 22-membered macrolide from a marine dinoflagellate *Amphidinium* species. Tetrahedron 70, 2962–2965.

Almandoz, G.O., Montoya, N.G., Hernando, M.P., Benavides, H.R., Carignan, M.O., Ferrario, M.E., 2014. Toxic strains of the *Alexandrium ostenfeldii* complex in southern South America (Beagle Channel, Argentina). Harmful Algae 37, 100–109.

Aráoz, R., Servent, D., Molgó, J., Iorga, B.I., Fruchart-Gaillard, C., Benoit, E., Gu, Z., Stivala, C., Zakarian, A., 2011. Pinnatoxins: an emergent family of marine phycotoxins targeting nicotinic acetylcholine receptors with high affinity. Toxins Ion Transf. 43–47.

Ben Naila, I., Hamza, A., Gdoura, R., Diogène, J., de la Iglesia, P., 2012. Prevalence and persistence of gymnodimines in clams from the Gulf of Gabes (Tunisia) studied by mouse bioassay and LC-MS/MS. Harmful Algae 18, 56–64.

Biré, R., Krys, S., Frémy, J.M., Dragacci, S., Stirling, D., Kharrat, R., 2002. First evidence on occurrence of gymnodimine in clams from Tunisia. J. Nat. Toxins 11, 269–275.

Cembella, A.D., Lewis, N.I., Quilliam, M.A., 2000. The marine dinoflagellate *Alexandrium ostenfeldii* (Dinophyceae) as the causative organism of spirolide shellfish toxins. Phycologia 39, 67–74.

Ciminiello, P., Dell'Aversano, C., Iacovo, E.D., Fattorusso, E., Forino, M., Grauso, L., Tartaglione, L., Guerrini, F., Pezzolesi, L., Pistocchi, R., 2010. Characterization of 27-hydroxy-13-desmethyl spirolide C and 27-oxo-13,19-didesmethyl spirolide C. Further insights into the complex Adriatic *Alexandrium ostenfeldii* toxin profile. Toxicon 56, 1327–1333.

de la Iglesia, P., McCarron, P., Diogène, J., Quilliam, M.A., 2013. Discovery of gymnodimine fatty acid ester metabolites in shellfish using liquid chromatography/mass spectrometry. Rapid Commun. Mass Spectrom. 27, 643–653.

EFSA Panel on Contaminants in the Food Chain (CONTAM), 2010. Scientific opinion on marine biotoxins in shellfish – cyclic imines (spirolides, gymnodimines, pinnatoxins and pteriatoxins) [39 pp.] EFSA J. 8 (6), 1628. http://dx.doi.org/10.2903/j.efsa.2010.1628. Available online: www.efsa.europa.eu.

García-Altares, M., Diogène, J., de la Iglesia, P., 2013. The implementation of liquid chromatography tandem mass spectrometry for the official control of lipophilic toxins in seafood: single-laboratory validation under four chromatographic conditions. J. Chromatogr. A 1275, 48–60.

Gerssen, A., Mulder, P.P.J., McElhinney, M.A., de Boer, J., 2009. Liquid chromatography-tandem mass spectrometry method for the detection of marine lipophilic toxins under alkaline conditions. J. Chromatogr. A 1216, 1421–1430.

Guéret, S.M., Brimble, M.A., 2010. Spiroimine shellfish poisoning (SSP) and the spirolide family of shellfish toxins: isolation, structure, biological activity and synthesis. Nat. Prod. Rep. 27, 1350–1366.

Guillard, R.R.L., Ryther, J.H., 1962. Studies of marine planktonic diatoms. I. *Cyclotella nana* (Hustedt) and *Detonula confervacea* (Cleve). Can. J. Microbiol. 8, 229–239.

Harris, R.K., Becker, E.D., Cabral De Menezes, S.M., Granger, P., Hoffman, R.E., Zilm, K.W., 2008. Further conventions for NMR shielding and chemical shifts: (IUPAC recommendations 2008). Pure Appl. Chem. 80, 59–84.

Hu, T., Curtis, J.M., Oshima, Y., Quilliam, M.A., Walter, J.A., Watson-Wright, W.M., Wright, J.L.C., 1995. Spirolides B and D, two novel macrocycles isolated from the digestive glands of shellfish. J. Chem. Soc. Chem. Commun. 2159–2161.

Hu, T., Burton, I.W., Cembella, A.D., Curtis, J.M., Quilliam, M.A., Walter, J.A., Wright, J.L.C., 2001. Characterization of spirolides A, C, and 13-desmethyl C, new marine toxins isolated from toxic plankton and contaminated shellfish. J. Nat. Prod. 64, 308–312.

Kellmann, R., Stüken, A., Orr, R.J.S., Svendsen, H.M., Jakobsen, K.S., 2010. Biosynthesis and molecular genetics of polyketides in marine dinoflagellates. Mar. Drugs 8, 1011–1048.

Kharrat, R., Servent, D., Girard, E., Ouanounou, G., Amar, M., Marrouchi, R., Benoit, E., Molgó, J., 2008. The marine phycotoxin gymnodimine targets muscular and neuronal nicotinic acetylcholine receptor subtypes with high affinity. J. Neurochem. 107, 952–963.

Kremp, A., Tahvanainen, P., Litaker, W., Krock, B., Suikkanen, S., Leaw, C.P., Tomas, C., 2014. Phylogenetic relationships, morphological variation, and toxin patterns in the *Alexandrium ostenfeldii* (Dinophyceae) complex: implications for species boundaries and identities. J. Phycol. 50, 81–100.

Kremp, A., Oja, J., LeTortorec, A.H., Hakanen, P., Tahvanainen, P., Tuimala, J., Suikkanen, S., 2016. Diverse seed banks favour adaptation of microalgal populations to future climate conditions. Environ. Microbiol. http://dx.doi.org/10.1111/1462-2920.13070.

MacKinnon, S.L., Walter, J.A., Quilliam, M.A., Cembella, A.D., LeBlanc, P., Burton, I.W., Hardstaff, W.R., Lewis, N.I., 2006a. Spirolides isolated from Danish strains of the toxigenic dinoflagellate *Alexandrium ostenfeldii*. J. Nat. Prod. 69, 983–987.

MacKinnon, S.L., Cembella, A.D., Burton, I.W., Lewis, N., LeBlanc, P., Walter, J.A., 2006b. Biosynthesis of 13-desmethyl spirolide C by the dinoflagellate *Alexandrium ostenfeldii*. J. Org. Chem. 71, 8724–8731.

McCarron, P., Wright, E., Quilliam, M.A., 2014. Liquid chromatography/mass spectrometry of domoic acid and lipophilic shellfish toxins with selected reaction monitoring and optional confirmation by library searching of product ion spectra. J. AOAC Int. 97, 316–324.

Miles, C.O., Wilkins, A.L., Stirling, D.J., MacKenzie, A.L., 2000. New analogue of gymnodimine from a *Gymnodinium* species. J. Agric. Food Chem. 48, 1373–1376.

Miles, C.O., Wilkins, A.L., Stirling, D.J., MacKenzie, A.L., 2003. Gymnodimine C, an isomer of gymnodimine B, from *Karenia selliformis*. J. Agric. Food Chem. 51, 4838–4840.

Molgó, J., Girard, E., Benoit, E., 2007. Cyclic imines: an insight into this emerging group of bioactive marine toxins. In: Botana, L.M. (Ed.), Phycotoxins: Chemistry and Biochemistry. Blackwell Publishing, Ames, Iowa, pp. 319–335.

Molgó, J., Aráoz, R., Iorga, B.I., Benoit, E., Zakarian, A., 2014. Cyclic imine neurotoxins acting on muscarinic and nicotinic acetylcholine receptors. In: Rossini, G.P. (Ed.), Toxins and Biologically Active Compounds from Microalgae. CRC Press, pp. 116–146.

Munday, R., Towers, N.R., MacKenzie, L., Beuzenberg, V., Holland, P.T., Miles, C.O., 2004. Acute toxicity of gymnodimine to mice. Toxicon 44, 173–178.

Munday, R., 2008. Toxicology of cyclic imines: gymnodimine, spirolides, pinnatoxins, pteriatoxins, prorocentrolide, spiro-prorocentrimine, and symbioimines. In: Botana, L.M. (Ed.), Seafood and Freshwater Toxins: Pharmacology, Physiology, and Detection, second ed. CRC Press, pp. 581–594.

Rhodes, L., Smith, K., Selwood, A., McNabb, P., van Ginkel, R., Holland, P., Munday, R., 2010. Production of pinnatoxins by a peridinoid dinoflagellate isolated from Northland, New Zealand. Harmful Algae 9, 384–389.

Rhodes, L., Smith, K., Selwood, A., McNabb, P., Munday, R., Suda, S., Molenaar, S., Hallegraeff, G., 2011. Dinoflagellate *Vulcanodinium rugosum* identified as the causative organism of pinnatoxins in Australia, New Zealand and Japan. Phycologia 50, 624–628.

Roach, J.S., LeBlanc, P., Lewis, N.I., Munday, R., Quilliam, M.A., MacKinnon, S.L., 2009. Characterization of a dispiroketal spirolide subclass from *Alexandrium ostenfeldii*. J. Nat. Prod. 72, 1237–1240.

Rundberget, T., Aasen, J.A.B., Selwood, A.I., Miles, C.O., 2011. Pinnatoxins and spirolides in Norwegian blue mussels and seawater. Toxicon 58, 700–711.

Salgado, P., Riobó, P., Rodríguez, F., Franco, J.M., Bravo, I., 2015. Differences in the toxin profiles of *Alexandrium ostenfeldii* (Dinophyceae) strains isolated from different geographic origins: evidence of paralytic toxin, spirolide, and gymnodimine. Toxicon 103, 85–98.

Seki, T., Satake, M., MacKenzie, L., Kaspar, H.F., Yasumoto, T., 1995. Gymnodimine, a new marine toxin of unprecedented structure isolated from New Zealand oysters and the dinoflagellate, *Gymnodinium* sp. Tetrahedron Lett. 36, 7093–7096.

Selwood, A.I., Miles, C.O., Wilkins, A.L., van Ginkel, R., Munday, R., Rise, F., McNabb, P., 2010. Isolation, structural determination and acute toxicity of pinnatoxins E, F and G. J. Agric. Food Chem. 58, 6532–6542.

Selwood, A.I., Wilkins, A.L., Munday, R., Shi, F., Rhodes, L.L., Holland, P.T., 2013. Portimine: a bioactive metabolite from the benthic dinoflagellate *Vulcanodinium rugosum*. Tetrahedron Lett. 54, 4705–4707.

Selwood, A.I., Wilkins, A.L., Munday, R., Gu, H., Smith, K.F., Rhodes, L.L., Rise, F., 2014. Pinnatoxin H: a new pinnatoxin analog from a South China Sea *Vulcanodinium rugosum* isolate. Tetrahedron Lett. 55, 5508–5510.

Sleno, L., Chalmers, M.J., Volmer, D.A., 2004. Structural study of spirolide marine toxins by mass spectrometry. Part II. Mass spectrometric characterization of unknown spirolides and related compounds in a cultured phytoplankton extract. Anal. Bioanal. Chem. 378, 977–986.

Stewart, M., Blunt, J.W., Munro, M.H.G., Robinson, W.T., Hannah, D.J., 1997. The absolute stereochemistry of the New Zealand shellfish toxin gymnodimine. Tetrahedron Lett. 38, 4889–4890.

Stirling, D.J., 2001. Survey of historical New Zealand shellfish samples for accumulation of gymnodimine. N. Z. J. Mar. Freshw. Res. 35, 851–857.

Suikkanen, S., Kremp, A., Hautala, H., Krock, B., 2013. Paralytic shellfish toxins or spirolides? The role of environmental and genetic factors in toxin production of the *Alexandrium ostenfeldii* complex. Harmful Algae 26, 52–59.

Tahvanainen, P., Alpermann, T.J., Figueroa, R.I., John, U., Hakanen, P., Nagai, S., Blomster, J., Kremp, A., 2012. Patterns of post-glacial genetic differentiation in marginal populations of a marine microalga. PLoS One 7, e53602.

Takada, N., Umemura, N., Suenaga, K., Uemura, D., 2001. Structural determination of pteriatoxins A, B and C, extremely potent toxins from the bivalve *Pteria penguin*. Tetrahedron Lett. 42, 3495–3497.

Thiele, C.M., Petzold, K., Schleucher, J., 2009. EASY ROESY: reliable cross-peak integration in adiabatic symmetrized ROESY. Chem. Eur. J. 15, 585–588.

Tillmann, U., Kremp, A., Tahvanainen, P., Krock, B., 2014. Characterization of spirolide producing *Alexandrium ostenfeldii* (Dinophyceae) from the western Arctic. Harmful Algae 39, 259–270.

Van de Waal, D.B., Tillmann, U., Martens, H., Krock, B., van Scheppingen, Y., John, U., 2015. Characterization of multiple isolates from an *Alexandrium ostenfeldii* bloom in The Netherlands. Harmful Algae 49, 94–104.

Van Wagoner, R.M., Misner, I., Tomas, C.R., Wright, J.L.C., 2011. Occurrence of 12-methylgymnodimine in a spirolide-producing dinoflagellate *Alexandrium peruvianum* and the biogenetic implications. Tetrahedron Lett. 52, 4243–4246.

Van Wagoner, R.M., Satake, M., Wright, J.L.C., 2014. Polyketide biosynthesis in dinoflagellates: what makes it different? Nat. Prod. Rep. 31, 1101–1137.

Vilotijevic, I., Jamison, T.F., 2010. Synthesis of marine polycyclic polyethers via endo-selective epoxide-opening cascades. Mar. Drugs 8, 763–809.

Wider, G., Dreier, L., 2006. Measuring protein concentrations by NMR Spectroscopy. J. Am. Chem. Soc. 128, 2571–2576.